

Modeling the Geometry of an Underwater Channel for Acoustic Communication

Hala A. Naman^{1,2} and A.E. Abdelkareem¹

¹College of Information Engineering, Al-Nahrain University, Iraq,

²College of Engineering, University of Wasit, Iraq

<https://doi.org/10.26636/jtit.2022.164822>

Abstract — The achievement of efficient data transmissions via underwater acoustic channels, while dealing with large data packets and real-time data fed by underwater sensors, requires a high data rate. However, diffraction, refraction, and reflection phenomena, as well as phase and amplitude variations, are common problems experienced in underwater acoustic (UWA) channels. These factors make it difficult to achieve high-speed and long-range underwater acoustic communications. Due to multipath interference caused by surface and ocean floor reflections, the process of modeling acoustic channels under the water's surface is of key importance. This work proposes a simple geometry-based channel model for underwater communication. The impact that varying numbers of reflections, low water depth values, and distances between the transmitter and the receiver exert on channel impulse response and transmission loss is examined. The high degree of similarity between numerical simulations and actual results demonstrates that the proposed model is suitable for describing shallow underwater acoustic communication environments.

Keywords — channel impulse response, geometry channel model, multipath propagation, underwater acoustic communication.

1. Introduction

Due to the increasing number of civilian and military applications of ocean monitoring solutions, underwater wireless communication has become, in recent years, a research domain with great prospects. Underwater acoustic channels are a difficult environment for ensuring reliable communications, due to the significant influence of multipath propagation, Doppler shifts, and high signal attenuation [1], [2]. Such parameters as efficiency and capacity of communication channels are affected by the abovementioned factors, as the time dispersion of the transmitted signal caused by multipath propagation leads to frequency-selective fading in the channel's frequency response. High frequencies are largely absorbed at large distances at the sea level, meaning they cannot be used in underwater channels. The usable band for underwater communications ranges from tens of Hz to 1 MHz, and this is why the vast majority of underwater communication signals are of the acoustic variety, since only such a solution is capable of working efficiently at distances of many kilometers [3]. Models highlighting the influence of real underwater envi-

ronment parameters on underwater acoustic channels serve as an efficient channel analysis method. A signal traveling from the source to the receiver does not always follow the shortest path available. Usually, it reflects from the bottom and the surface of the water, meaning that it suffers from refraction caused by propagation speed differences [4]. Therefore, the received signal is influenced by the presence of its multiple delayed replicas, a phenomenon known as inter-symbol interference (ISI). In addition, significant multipath signal amplitude causes serious signal corruption-related issues in the case of signals propagating in shallow water [5], [6]. Consequently, the modeling an underwater transmission system's channel is necessary for analyzing the multipath phenomena and for coming up with effective solutions facilitating underwater acoustic communication.

2. Related Work

Paper [7] proposes a simple, effective, geometry-based channel model for time-reversal communication by analyzing transmitter and receiver height at different distances. This research also proposes time reversal and OFDM communication, which work together rather well. According to simulations, TR-OFDM can produce a BER of less than 0.001 at SNR exceeding 10 dB. In [8], a geometry-based model is developed to represent multipath scattering between the transmitter and the receiver. Such an approach allows to explore the impact of scattering environments on propagation characteristics with minimum complexity, by using a rectangle to characterize the communication environments of the ocean's vertical cross section, where scatterers are randomly distributed on the surface and on the bottom. In [9], the angle of arrival distribution has been calculated for the propagation path model in a UW channel that experiences incoherent scattering from the surface and the bottom. The scattering would be directed for the medium frequency range and an acoustically flat surface/bottom. Incoherent scattering significantly contributes to the scattered field with high-frequency acoustic waves or rough boundaries. This approach has the potential to aid the development of precise and cost-effective systems for high-frequency communication between mobile UW and surface platforms. Paper [10] proposed a non-stationary wide-

band channel model for UWA in shallow water. Multiple motion effects, time-varying angles, distances, cluster locations with channel geometry, and ultra-wideband properties are incorporated in this geometry-based stochastic model, making it more realistic and capable of sustaining long time/distance simulations.

This paper proposes a simple time-varying geometry model using a triangle concept to define the characteristics of a shallow underwater acoustic channel environment. Assuming that the multipath is randomly distributed on the sea's surface and bottom, the direct path components propagate by reflections on the sea surface, and multipath components propagate by reflections on the sea floor. Finally, all of them come together to form the proposed model. Channel impulse response and transmission loss are considered in the proposed model as well.

This paper is organized as follows: Section 3 describes the theory of channel characteristics used in UWA communication. The proposed geometry channel model is shown in Section 4. Section 5 compares the proposed model with the Bellhop simulator result and shows simulation results. Section 6 presents the paper's final findings and discussions.

3. Channel Characteristics in UWA Communication

To introduce the basic channel model, it is necessary to understand its properties, such as delay of propagation, absorption, spreading loss, and transmission loss. The Doppler effect and inter-symbol interference (ISI) take place, since the channel has a time-varying multipath, delays disperse over 100 symbol times, and the acoustic speed is slow [11]. Figure 1 depicts the architecture of this propagation model. In this case, it is assumed that the propagation vibrations are a combination of direct path reflections and multipath reflections. Because of bandwidth limitations, the parameters of the signal's sensitivity to such a multipath propagation environment change with time and vary at transmitter and receiver positions. Vertical and horizontal connection configurations are the primary factors taken into consideration while establishing the rate of multipath propagation [12]. On the other hand, multipath spreading in horizontal channels might be substantially longer than those in vertical ones. This initial sea surface reflection is shown in green in Fig. 1. The red line represents the first shallow water bottom reflection of two forms of reflection.

Transmission loss (TL) characterizes the decay of signal intensity with increasing distance. Such parameters as total spreading and attenuation loss are used to determine this value, as demonstrated in Eq. (1) in [13]. During propagation, the inevitable frictional conversion of sound converts it into heat.

$$TL(f) = 2\alpha_z + k \log(r) + a(f)r. \quad (1)$$

As both the transmitter and receiver are toroidal beam-shaped transducers, attenuation α_z in the $z - y$ and $z - x$ planes is fixed at 15 dB, r is the propagation range in meters and k

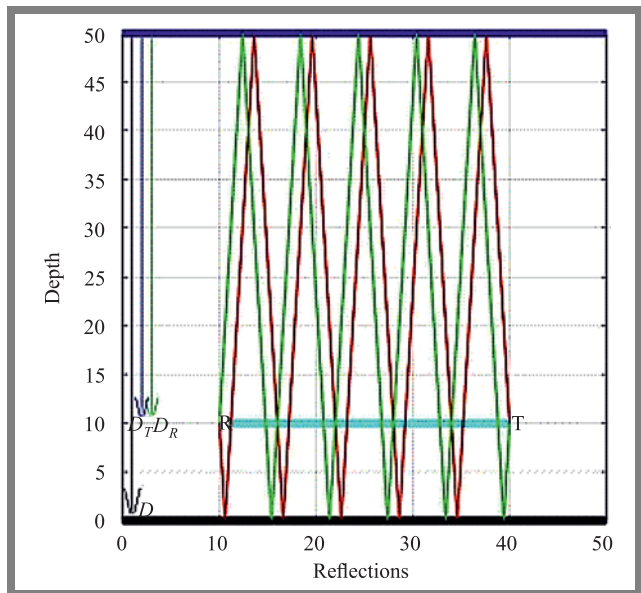


Fig. 1. Multipath reflection phenomena scheme in the communication channel.

represents the spreading factor selected describing the spreading loss. Spherical or cylindrical spreading determines the spreading loss in the second part of Eq. (1). When the boundaries of all reflected waves are far away from the transmitter and the receiver, meaning that no channeling of acoustic energy can occur, we say that the sound has spread spherically. In shallow water, this impact may be higher at higher frequencies because of the frequency-dependent attenuation per unit of distance. At $k = 20$, the fundamental loss law for spherical spreading is the “inverse-square law” which defines intensity $I(r)$ at range r as a percentage of the intensity at the standard reference range of 1 m. When the sea acts as an acoustic waveguide due to surface and seafloor reflections, spherical propagation conditions no longer apply. In this case, propagation may be defined according to the cylindrical spreading law, with $k = 10$. Considering that the boundary reflections are highly dependent on both the state of the sea and the characteristics of the bottom material, and that low-frequency sound travels very well through the sea floor, the cylindrical law is designed to be conservative in estimating losses. A useful rule is to adopt $k = 15$, i.e. a value at which an equidistant point between the spherical and cylindrical laws exists.

The third part of Eq. (1) represents attenuation in the sea – a phenomenon caused mainly by viscous friction, occurring at frequencies exceeding 1 MHz. At lower frequencies, molecular resonance results in the fact that attenuation of sea water is lower than that of purified water. Magnesium sulfate present in the sea water solution causes additional attenuation below 500 kHz, beyond the loss in pure water, finally increasing its level by a factor of approx. 18 for frequencies lower than 70 kHz. In spite of its negligible concentration in water, boric acid reliably boosts the loss at frequencies of less than 700 Hz, by a factor of 16. Based on those relations, Eqs.

(2)–(10) are used to determine $\alpha(f)$ [13]:

$$\alpha(f) = \alpha_1 + \alpha_\alpha + \alpha_3, \quad (2)$$

where:

$$\alpha_1 = af^2 \quad (\text{fresh water attenuation}), \quad (3)$$

$$\alpha_2 = \frac{bf_0}{(1 + (f_0/f)^2)} \quad (\text{magnesium sulfate relaxation}), \quad (4)$$

$$\alpha_3 = \frac{cf_1}{(1 + (f_1/f)^2)} \quad (\text{boric acid relaxation}), \quad (5)$$

$$a = 1.3 \times 10^{-7} + 2.1 \times 10^{-10}(T - 38^\circ)^2, \quad (6)$$

$$b = 2S \times 10^{-5}, \quad (7)$$

$$f_0 = 50 \times (T + 1), \quad (8)$$

$$c = 1.2 \times 10^{-4}, \quad (9)$$

$$f_1 = (10)^{(T-4)/100}. \quad (10)$$

Salinity is denoted by S , temperature by T [$^\circ\text{C}$], and frequency is denoted by f [kHz].

4. Proposed Geometry Channel Model

The proposed geometry-based propagation model uses a triangle concept to represent the various contexts of communication pertaining to shallow water propagation channels. It assumes that multipath reflection occurs randomly at the sea surface and at various depths. Direct path propagation delay T_D is determined by using the velocity formula $v = d/t$ where v denotes the velocity, d indicates the displacement, and t refers to the time:

$$T_D = (D_T - D_R)/c, \quad (11)$$

where the depth of the transmitter is D_T , the depth of the receiver is D_R , and c denotes the speed of sound. This model assumes that the D_R parameter is not constant and its value is relative to D_T . The angle $\theta = 90^\circ$ is between a column of water and the horizontal direction between the transmitter and receiver, as shown in Fig. 2.

First, by connecting T and R points with L , we get a right-sided triangle. Next, using the definition of cosine, D_R can be determined:

$$D_R = D_T - L \cdot \cos(\theta), \quad (12)$$

where L is the distance between the transmitter and the receiver.

According to Fig. 3, the delay in transmission between the transmitter and the receiver may be calculated using the Pythagorean theorem of right triangles, whether the signal is traveling over a straight path or a multipath. In this case, the hypotenuse reflects the time it takes for each reflection to complete its propagation. There are two types reverberations: surface reflections, in which the initial reflection occurs on the surface, and bottom reflections, in which the initial reflection occurs on the sea floor.

In the constructed triangle, d_1 is the propagation range created by the initial reflection between the transmitter and the surface. The magnitude of the vertical motion on the first reflection line segment is equal to D_T and next to receiver R via d_2 .

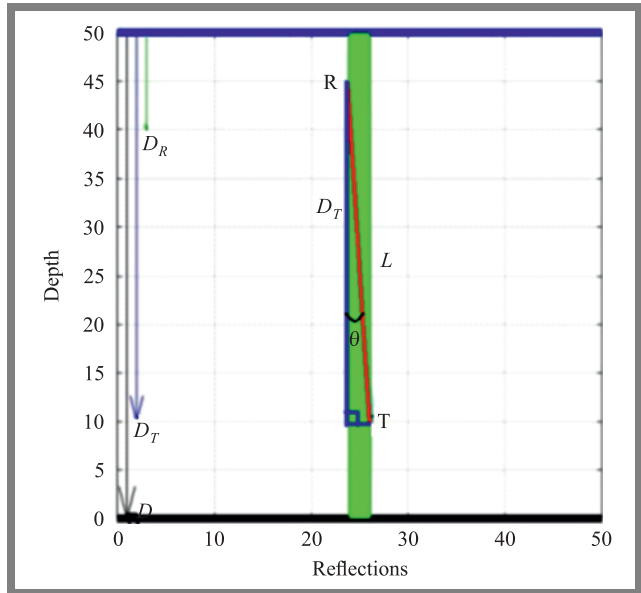


Fig. 2. Method for determining receiver depth.

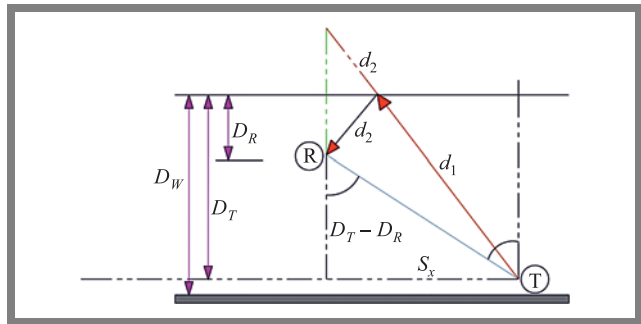


Fig. 3. Pythagorean theorem used for determining multipath surface reflections.

The magnitude of the vertical motion on the second reflection line segment is D_R . After drawing the reflected distance, d_2 is supplied to d_1 as an extension. So, the sum of the vertical motion on these two segments d_1 and d_2 is $D_T + D_R$. The side designated by S_y is perpendicular to the hypotenuse, while the side designated by S_x is next to it:

$$S = \sqrt{S_x^2 + S_y^2}, \quad (13)$$

$$S_y = D_T + D_R. \quad (14)$$

The method of calculating S_x is depicted in Fig 3. Let us consider two transient vertical line segments from points T and R that are parallel to each other and are intersected by a blue diagonal line. The resulting angles will be equal in pairs (alternate angles), i.e. $\theta = \theta_1$ and:

$$\begin{aligned} \theta_1 + \theta_2 &= 90^\circ \implies \theta_1 = 90^\circ - \theta_2, \\ \text{tg}(\theta - 1) &= \frac{\sin(\theta - 1)}{\cos(\theta_1)} = \frac{\cos(90^\circ - \theta_2)}{\sin(90^\circ - \theta_2)} \\ &= \text{ctg}(90^\circ - \theta_2) = \text{ctg}(\theta_2), \end{aligned}$$

$$\text{ctg}(\theta_2) = \frac{S_x}{D_t - D_r},$$

$$\theta = \theta_1 \implies \text{tg}(\theta) = \frac{S_x}{D_t - D_r},$$

$$S_x = (D_T - D_R) \text{tg}(\theta). \quad (15)$$

For the two reflections ($N = 2$), the multipath propagation is represented in Fig. 4.

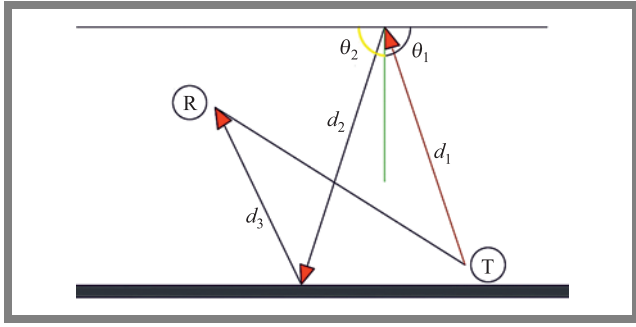


Fig. 4. Multipath propagation for $N = 2$.

During multipath propagation, S_x is unaffected by reflections, whereas S_y varies, which results in an increase of d_1 , d_2 and d_3 . Suppose θ_1 and θ_2 are two consecutive reflection angles, d_1 with θ_1 and d_2 with θ_2 are trigonometric pairs, such that:

$$\begin{aligned} \theta_2 &= 180^\circ - \theta_1 \implies \sin(\theta_2) = \sin(\theta_1) \text{ and } \cos(\theta_2) \\ &= -\cos(\theta_1), \end{aligned}$$

$$\text{tg}(\theta_2) = -\text{tg}(\theta_1) \implies m(d_2) = -m(d_1),$$

where θ_1 and θ_2 are two arbitrary consecutive reflection angles. Then:

$$\forall i \in \mathbb{N} m(d_{i+1}) = -m(d_i).$$

Both consecutive reflection lines have the same slope as the opposite sign. Suppose $m(d_i)$ represents the slope of d_i and:

$$\begin{aligned} \forall i \in \mathbb{N} |m(d_{i+1})| &= |m(d_i)|, \\ \forall i \in \mathbb{N} m(d_{i+2}) &= m(d_i), \\ \forall i \in \mathbb{N} \forall j \in \mathbb{N} |m(d_i)| &= |m(d_j)|, \\ \forall i \in \mathbb{N} |m(d_i)| &= |m(d_1)|. \end{aligned}$$

All the reflection lines are along the first reflection line, thus allowing to create vector \mathbf{S} that moves horizontally and vertically, as shown in Fig. 5.

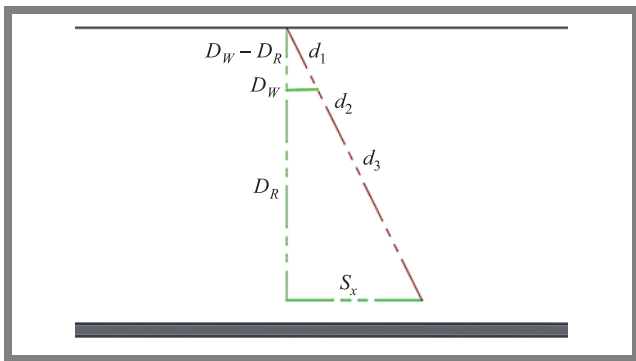


Fig. 5. Equivalent model for multipath propagation for $N = 2$.

For any number of surface reflections n (between 1 and N), the propagation delay is:

$$S_{y_n} = D_T + \left\lfloor \frac{n}{2} \right\rfloor 2D_W + (-1)^{n+1} D_R, \quad (16)$$

where D_W is the water depth.

Suppose n increases by two units. Therefore, two consecutive reflection vectors with opposite slopes are added to the previous set of reflections. The first reflection vector coming from the sea level to the depth and the second reflection vector going from the depth to the sea level. Each of these two shifts by D_W on the vertical axis. Hence, total displacement increases by $2D_W$, as shown in Fig. 6.

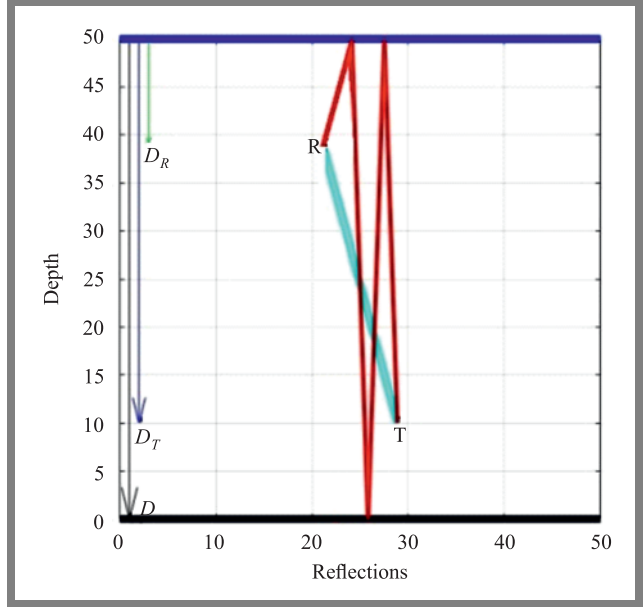


Fig. 6. Surface reflections when $N = 3$.

$$S_{y_{n+2}} = S_{y_n} + 2D_W \quad (N = 3),$$

$$S_{y_{n+2}} = D_T + \left\lfloor \frac{n}{2} \right\rfloor 2D_W + (-1)^{n+1} D_R + 2D_W,$$

$$S_{y_{n+2}} = D_T + \left(\left\lfloor \frac{n}{2} \right\rfloor + 1 \right) 2D_W + (-1)^{n+1} D_R,$$

$$S_{y_{n+2}} = D_T + \left\lfloor \frac{n+2}{2} \right\rfloor 2D_W + (-1)^{n+1} D_R.$$

Using induction on a natural odd number:

$$\forall n \in \mathbb{N}_O, S_{y_n} = D_T + \left\lfloor \frac{n}{2} \right\rfloor 2D_W + (-1)^{n+1} D_R.$$

Suppose $n = 2$, as shown in Fig. 7. From Eq. (16):

$$S_{y_2} = D_T + \left\lfloor \frac{2}{2} \right\rfloor 2D_W + (-1)^{2+1} D_R,$$

$$S_{y_2} = D_T + 2D_W + (-1^3 D_R),$$

$$S_{y_2} = D_T + 2D_W - D_R.$$

Assume n is an even natural number, i.e. $n \in \{2, 4, 6, \dots\}$. If S_{y_n} is correct, $S_{y_{n+2}}$ also is a correct formula.

$$S_{y_n} = D_T + \left\lfloor \frac{n}{2} \right\rfloor 2D_W + (-1)^{n+1} D_R.$$

Now suppose n increases by another two units. Consequently, two consecutive reflection vectors with opposite slopes are added to the previous set of reflections. The first reflection vector coming from the sea level to the depth and the second reflection vector going from the depth to the sea level. Each of these two shifts by D_W on the vertical axis and total displacement increases by $2D_W$ on the vertical axis, as shown in Fig. 8.

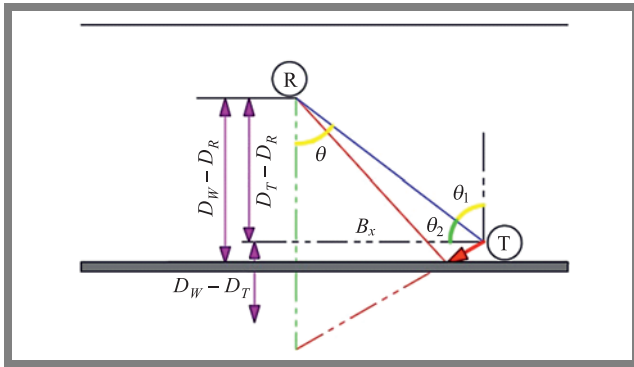


Fig. 10. Alternate angles for B_x calculation.

For any number of bottom reflections n , the propagation delay is:

$$B_{y_n} = \left\lceil \frac{n}{2} \right\rceil 2D_W - (D_T + -1^{n+1}D_R). \quad (21)$$

If n increases by two units, two consecutive reflection vectors with opposite slopes are added, as shown in Fig. 11. The first reflection vector is coming from the sea level to the depth of the sea and the other reflection vector is going from the depth to the sea level. Each of these two shifts by D_W on the vertical axis. So, total displacement increases by $2D_W$ on the vertical axis.

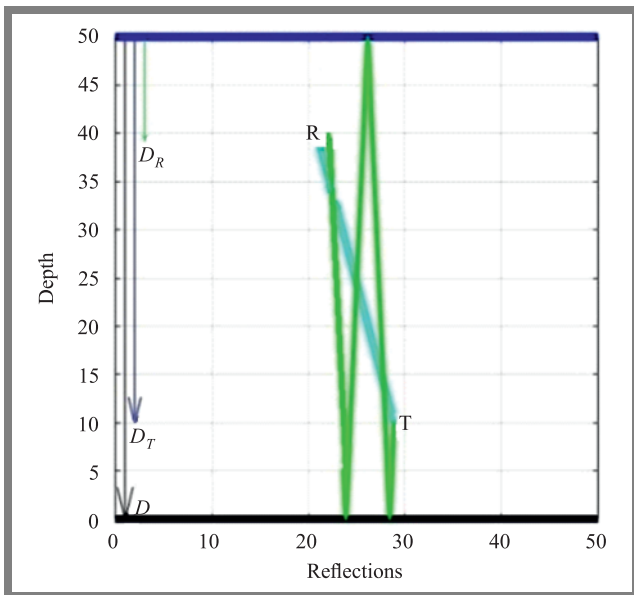


Fig. 11. Bottom reflection for $N = 3$.

$$B_{y_{n+2}} = B_{y_n} + 2D_W,$$

$$B_{y_{n+2}} = \left(\left\lceil \frac{n}{2} \right\rceil 2D_W \right) - (D_T + -1^{n+2+1}D_R) + 2D_W,$$

$$B_{y_{n+2}} = \left\lceil \frac{n+2}{2} \right\rceil 2D_W - (D_T + -1^{n+1}D_R),$$

Suppose n increases by another two units (Fig. 12).

Similarly, each of these two moves by D_W on the vertical axis and total displacement increases by $2D_W$ on the vertical axis.

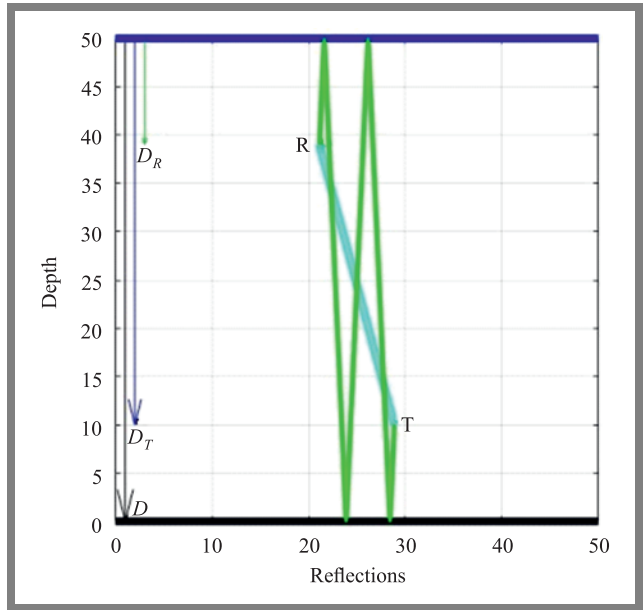


Fig. 12. Bottom reflection when $N = 4$.

$$B_{y_{n+2}} = B_{y_n} + 2D_W,$$

$$B_{y_{n+2}} = \left(\left\lceil \frac{n}{2} \right\rceil 2D_W \right) - (D_T + -1^{n+2+1}D_R) + 2D_W,$$

$$B_{y_{n+2}} = \left\lceil \frac{n+2}{2} \right\rceil 2D_W - (D_T + -1^{n+1}D_R).$$

The propagation delay for any number of reflections is:

$$B = \sqrt{B_x^2 + B_y^2} = \quad (22)$$

$$= \sqrt{((D_T - D_R) \text{tg} \theta)^2 + \left(\left\lceil \frac{n}{2} \right\rceil 2D_W - (D_T + -1^{n+1}D_R) \right)^2}$$

$$T_{Bn} = \frac{B}{c} = \frac{\sqrt{(D_T - D_R)^2 \text{tg}^2 \theta + \left(\left\lceil \frac{n}{2} \right\rceil 2D_W - (D_T + -1^{n+1}D_R) \right)^2}}{c}$$

The main equation of channel impulse response (CIR) representing a multipath channel can be modeled as:

$$h(\tau, t) = \sum_{l=1}^L h_l(t) \delta[t - \tau_l(t)], \quad (23)$$

where $h_l(t)$ represents the path amplitudes, $\tau_l(t)$ denotes the time-varying path delays based on the proposed model and L is the total number of paths.

5. Simulation Results

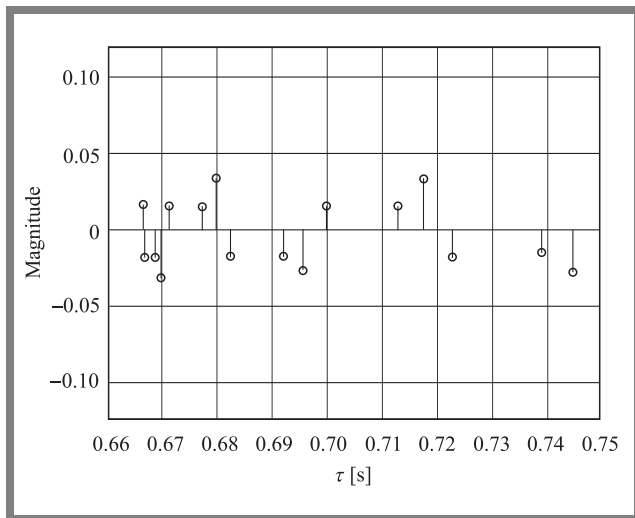
This section presents the results of a simulation performed with the use of Matlab for the proposed channel model. Table 1 presents the simulation parameters.

Normal incident waves at the sea surface border create a pressure reflection coefficient of -1 , while waves reflected from the sea floor have a pressure reflection coefficient of approx. 1 [14]. Even surface reflections add up constructively at the receiver side, while odd surface and bottom reflections add up destructively.

Tab. 1. Simulation parameters.

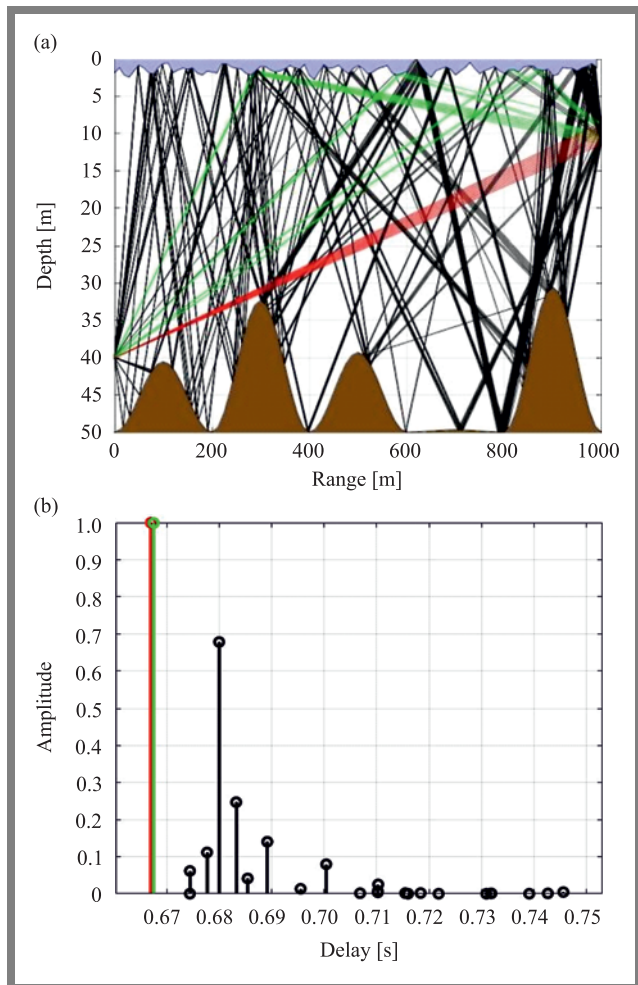
Parameter	Value
Transmitter depth	40 m
Receiver depth	Related to transmitter depth – Eq. (12)
Temperature	14°C
Salinity	35
Frequency	12 kHz
Spreading factor	15

The multipath channel between the source and the receiver is shown in Fig. 13 as a communication channel response. The delay spread of the reverberations in the communication channel equaled up to 79 ms.


Fig. 13. Communication CIR with $D_W = 50$ and $L = 1000$.

To evaluate the performance of the proposed model, the same configuration parameters (D_W, D_R, D_T, L, f) were implemented in the Bellhop simulator [15] as indicated in Fig. 14. Here, the red path shows the direct path or a signal that begins at the sea floor and gradually refracts upwards or diverges upwards until a steep positive sound speed gradient is met, at which point it refracts downward. The green path of the signal reaches the receiver via a reflection from the water surface and/or bottom. Black paths refer to multiple multipath components arriving at the receiver due to the increased variety of potential paths reflected off the sea surface and an uneven sea bottom. Comparison of the delay spread achieved by the newly proposed model (79 ms) and the results of the Bellhop simulator [15] (78 ms) shows that the results are very close. The difference stems from the number of reflections used to represent the propagation delay.

When simulating the proposed model at different water depths, it was found that the multipath propagation effect increases with depth. As shown in Fig. 15, the delay spread for depths of 50, 100, 150, and 200 m equals 79, 279, 535, and 824 ms, respectively. Reflection of sound at the surface and bottom and its refraction caused by spatial variation in the speed of sound in water is responsible for multipath propagation. The speed of sound varies with temperature and pressure.


Fig. 14. Underwater multipath propagation environment obtained with the Bellhop simulator: a) ray trace, b) CIR.

For a depth of 50–100 m, the speed of sound remains constant, while at a depth of 150–200 m, the water temperature is lower, and therefore the speed of sound decreases.

Next, the simulations verified different distances between the transmitter and the receiver. Here, the highest delay spread for channel lengths of 500 and 1000 m was 138 and 79 ms, respectively. However, the 500 m CIR appears to be more severe, because some of its paths have a similar amplitude to the direct path, and the delay spread is longer, as shown in Fig. 16.

The transmission and reflection losses in sea water were then researched in a geometry model to describe CIR taps. It was shown that the model adequately captured the characteristics of the communication channel. In Figs. 17–18, the transmission loss increased with more multipath reflections and the growing communication distance, reaching more than 81 dB and 78 dB, respectively. The transmission loss depends on how the propagation of sound changes from spherical to cylindrical propagation. Moreover, attenuation increases with the communication distance which, in turn, increases the power loss. In shallow waters with a boundary formed by the sea floor, the grazing angle is affected as well. Figures 17–18 show that the transmission loss of the communication chan-

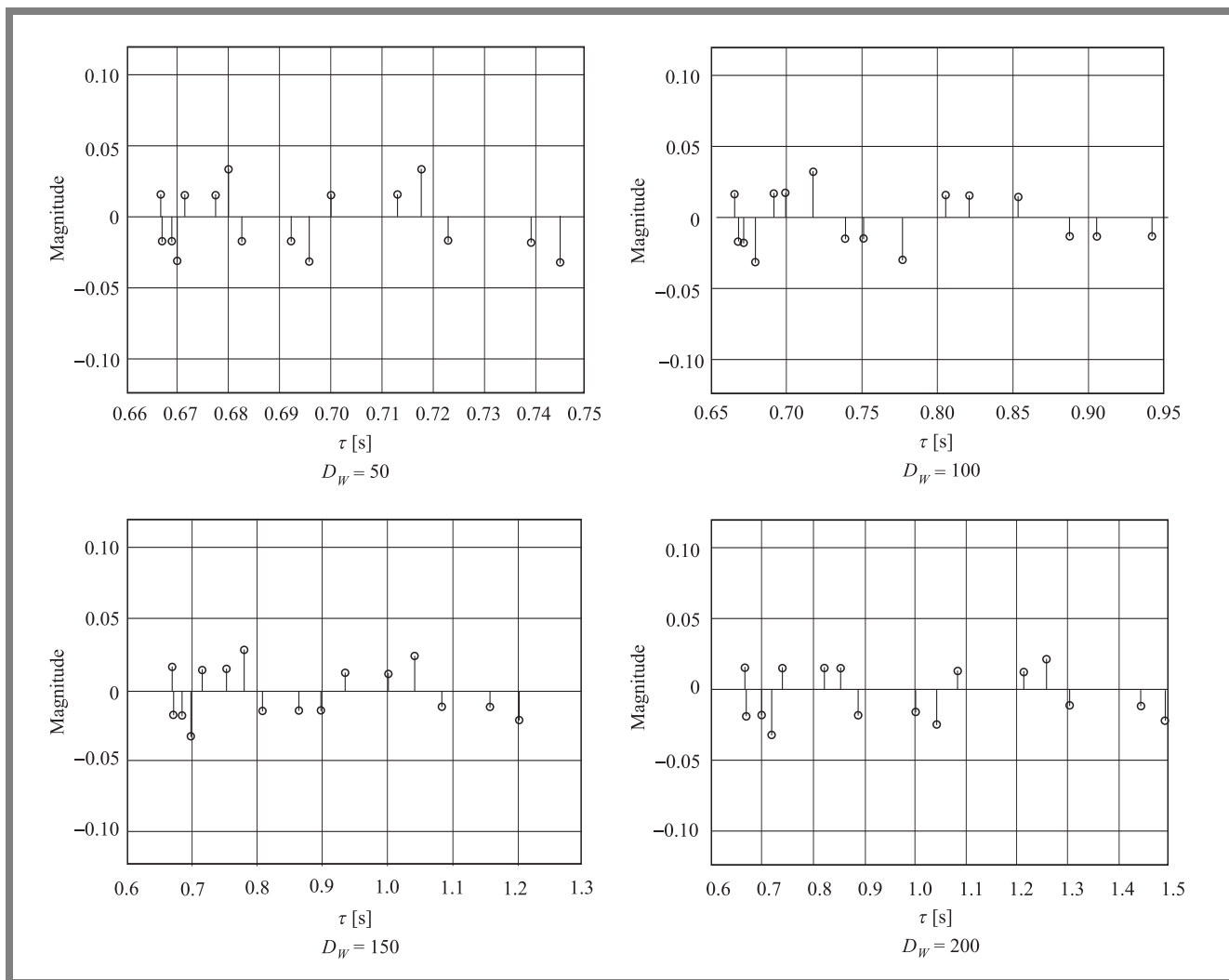


Fig. 15. Communication channel impulse response for $N = 20$ and $L = 1000$ with different water depths.

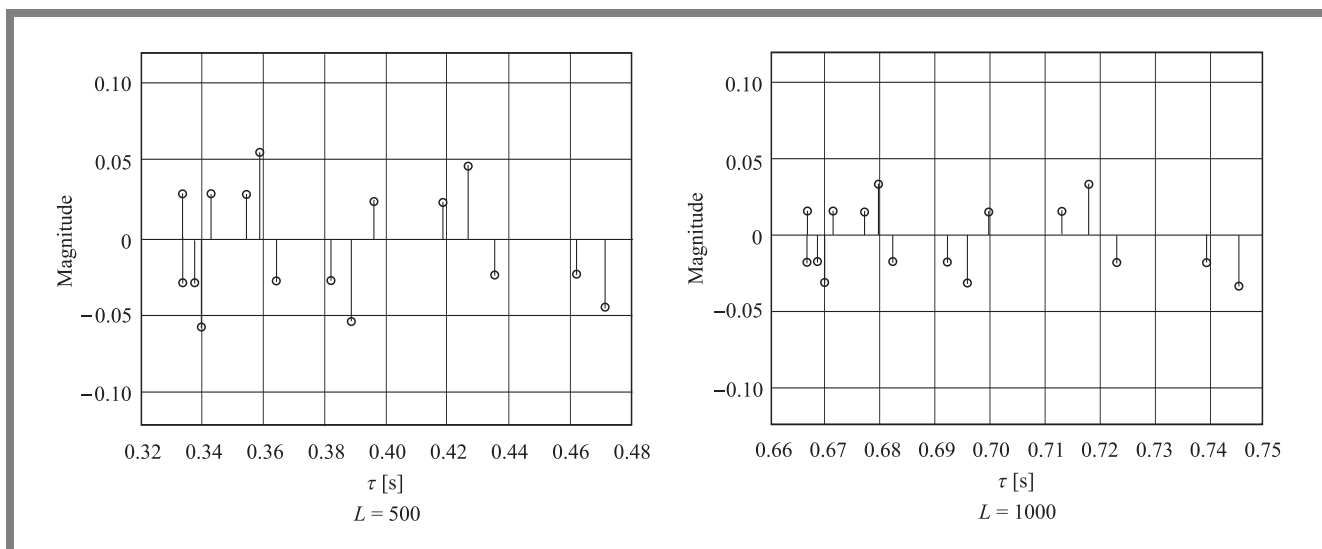


Fig. 16. Communication channel impulse response with $D_W = 50$ and different L values.

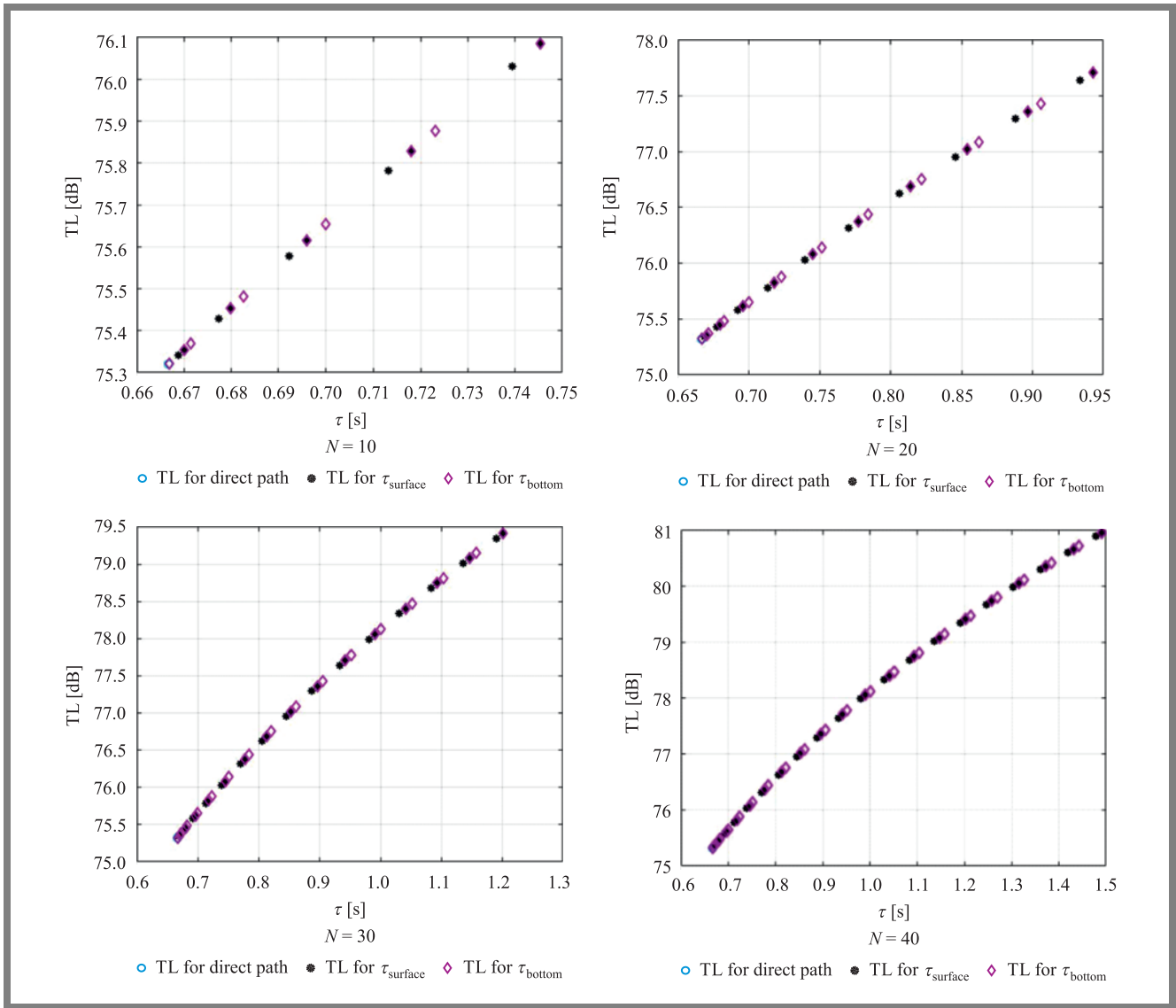


Fig. 17. Transmission loss of the communication channel with $L = 1000$, $D_W = 50$ with varying number of reflections.

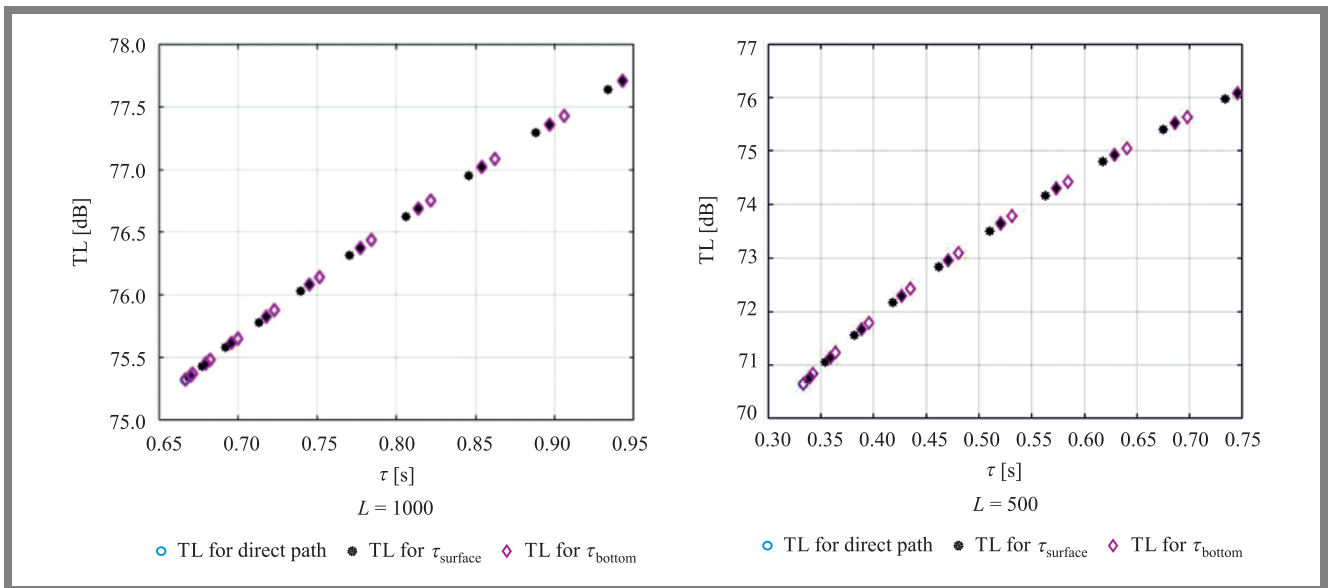


Fig. 18. Transmission loss of communication channel with $D_W = 50$ and different L .

nel increases with the growing number of reverberations and the communication distance.

6. Conclusions

This paper presents a geometric model of an underwater communication channel environment for multipath propagation delay simulations based on the triangle concept. It describes the multipath effect caused by surface and bottom reverberations and determines the communication channel's impulse response by changing the underwater depth and communication distance. The simulation results show that when the communication distance and the number of reflections from the surface and the bottom increase, the propagation losses increase as well. Comparisons of the propagation delay identified in the course of the simulations and the traditional results confirm that the proposed model successfully describes the communication channel's behavior in a shallow water scenario.

References

- [1] M. Stojanovic and J. Preisig, "Underwater Acoustic Communication Channels: Propagation Models and Statistical Characterization", *IEEE Commun. Mag.*, vol. 47, no. 1, pp. 84–89, 2009 (DOI: 10.1109/MCOM.2009.4752682).
- [2] A. E. Abdelkareem, B.S. Sharif, C.C. Tsimenidis, and J.A. Neasham, "Time Varying Doppler-Shift Compensation for OFDM-Based Shallow Underwater Acoustic Communication Systems", *2011 IEEE Eighth International Conference on Mobile Ad-Hoc and Sensor Systems*, 2011, pp. 885–891 (DOI: 10.1109/MASS.2011.105).
- [3] B.J. Heidemann, M. Stojanovic, and M. Zorzi, "Underwater sensor networks: applications, advances and challenges", *Trans. R. Soc. A*, vol. 370, pp. 158–175, 2012 (DOI: 10.1098/rsta.2011.0214).
- [4] J. Hui and X. Sheng, "Reverberation Channel", *Underwater Acoustic Channel*, Singapore: Springer Nature Singapore, 2022, pp. 175–191 (DOI: 10.1007/978-981-19-0774-6).
- [5] R.F. Coates, "Underwater acoustic communication", *Sea Technol.*, vol. 35, no. 7, pp. 41–47, 1994 (URL: https://archive.org/details/sim_sea-technology_1994-07_35_7/page/n3/mode/2up).
- [6] M. Elamassie, F. Miramirkhani, and M. Uysal, "Channel modeling and performance characterization of underwater visible light communications", *2018 IEEE Int. Conf. Commun. Work. ICC Work, 2018 – Proc.*, pp. 1–5, 2018 (DOI: 10.1109/ICCW.2018.8403731).
- [7] Y. Widiarti, Suwadi, Wirawan, and T. Suryani, "A Geometry-Based Underwater Acoustic Channel Model for Time Reversal Acoustic Communication", *Proceeding – 2018 Int. Semin. Intell. Technol. Its Appl. ISITIA 2018*, pp. 345–350, 2018 (DOI: 10.1109/ISITIA.2018.8711067).
- [8] J. Zhou, H. Jiang, P. Wu, and Q. Chen, "Study of Propagation Channel Characteristics for Underwater Acoustic Communication Environments", *IEEE Access*, vol. 7, pp. 79438–79445, 2019 (DOI: 10.1109/ACCESS.2019.2921808).
- [9] M. Rawat, B. Lall, and S. Srirangarajan, "Angle of Arrival Distribution in an Underwater Acoustic Communication Channel with Incoherent Scattering", *IEEE Access*, vol. 8, pp. 133204–133211, 2020 (DOI: 10.1109/ACCESS.2020.3008602).

- [10] X. Zhu, C. X. Wang, and R. Ma, "A 2D Non-Stationary Channel Model for Underwater Acoustic Communication Systems", *IEEE Veh. Technol. Conf.*, vol. 2021-April, pp. 0–5, 2021 (DOI: 10.1109/VTC2021-Spring51267.2021.9448976).
- [11] A.E. Abdelkareem, B.S. Sharif, and C. C. Tsimenidis, "Adaptive time varying Doppler shift compensation algorithm for OFDM-based underwater acoustic communication systems", *Ad Hoc Networks*, vol. 45, pp. 104–119, 2016 (DOI: 10.1016/j.adhoc.2015.05.011).
- [12] Y. Lou and N. Ahmed, "Basic Principles of Underwater Acoustic Communication", *Underwater Communications and Networks, Cham: Springer International Publishing*, pp. 3–33, 2022 (DOI: 10.1007/978-3-030-86649-5_1).
- [13] R.F. W. Coates, "Underwater Acoustic Systems", Wiley, 1990 (ISBN: 9780470215449).
- [14] D. Porta, "Underwater acoustic communications", *Sea Technol.*, vol. 39, no. 2, pp. 49–55, 1998 (URL: https://archive.org/details/sim_sea-technology_1998-02_39_2/page/n3/mode/2up).
- [15] N. Morozs *et al.*, "Channel Modeling for Underwater Acoustic Network Simulation", no. June, pp. 1–25, 2020 (DOI: 10.1109/ACCESS.2020.3011620).



Hala A. Naman received the B.Sc. and M.Sc. degrees in computer engineering from the University of Technology, Baghdad, Iraq, in 2001 and 2014, respectively. Currently, she is a Ph.D. candidate in Information and Communication Engineering at Al-Nahrain University, Iraq, and is a working lecturer college of engineering at the University of Wasit, Iraq. Her research interests include image processing, computer network, and signal processing for underwater communications.
E-mail: haltaee@uowasit.edu.iq
College of Information Engineering. Al-Nahrain University, Iraq
College of Engineering. University of Wasit, Iraq



A.E. Abdelkareem received the B.Sc. and M.Sc. degrees in computer engineering from the University of Technology, Baghdad, Iraq, in 1992 and 2002, respectively. He received the Ph.D. degree from Newcastle University, England, 2012. Currently, he is working lecturer at Al-Nahrain University, Iraq. His research interests include computer architectures, signal processing for underwater communications, digital signal processors, WSN and Internet of underwater things and embedded systems using SHARC processor.
E-mail: Ammar.algassab@nahrainuniv.edu.iq
College of Information Engineering. Al-Nahrain University, Iraq